Materials Physics and Mechanics 19 (2014) 51-67 Received: April 1, 2014

FLEXURAL WAVE MOTION IN A HEAT CONDUCTING DOUBLY CONNECTED THERMO-ELASTIC PLATE OF POLYGONAL CROSS-SECTIONS

R. Selvamani

Department of Mathematics, Karunya University, Coimbatore, Tamil Nadu, India

*e-mail: selvam1729@gmail.com

Abstract. Flexural wave motion in a heat conducting thermo elastic doubly connected polygonal plate is studied by using the Fourier expansion collocation method. The equations of motion based on two-dimensional theory of elasticity is applied under the plane strain assumption of generalized thermo elastic plate of polygonal cross-sections composed of homogeneous isotropic material. The frequency equations are obtained by satisfying the boundary conditions along the inner and outer surface of the polygonal plate. The numerical calculations are carried out for triangular, square, pentagonal and hexagonal cross sectional plates. The computed non-dimensional frequencies are compared with the Lord-Shulman (LS), Green-Lindsay (GL), coupled Theory (CT) theories of thermo-elasticity and they are presented in Tables. The dispersion curves are drawn for non-dimensional frequencies of thermally insulated and isothermal boundaries.

1. Introduction

The propagation of waves in thermo elastic materials has many applications in various fields of science and technology, namely, atomic physics, industrial engineering, thermal power plants, submarine structures, pressure vessel, aerospace, chemical pipes, and metallurgy. The importance of thermal stresses in causing structural damages and changes in functioning of the structure is well recognized whenever thermal stress environments are involved. Therefore, the ability to predict elastodynamics stresses induced by sudden thermal loading in composite structures is essential for the proper and safe design and the knowledge of its response during the service in these severe thermal environments.

A method, for solving wave propagation in arbitrary and polygonal cross-sectional plates and to find out the phase velocities in different modes of vibrations namely longitudinal, torsional and flexural, by constructing frequency equations was devised by Nagaya [1-5]. He formulated the Fourier expansion collocation method for this purpose and the same method is used in this problem. The generalized theory of thermo elasticity was developed by Lord and Shulman [6] involving one relaxation time for isotropic homogeneous media, which is called the first generalization to the coupled theory of elasticity. These equations determine the finite speeds of propagation of heat and displacement distributions, the corresponding equations for an isotropic case were obtained by Dhaliwal and Sherief [7]. The second generalization to the coupled theory of elasticity is what is known as the theory of thermo elasticity, with two relaxation times or the theory of temperature-dependent thermoelectricity. A generalization of this inequality was proposed by Green and Laws [8]. Green and Lindsay [9] obtained an explicit version of the constitutive equations. These equations were also obtained independently by Suhubi [10]. This theory contains two constants that act as relaxation times and modify not only the heat equations, but also all the equations of the coupled theory. The classical Fourier's law of heat conduction is not violated if the medium under consideration has a center of symmetry. Erbay and Suhubi [11] studied the longitudinal wave propagation in a generalized thermoplastic infinite cylinder and obtained the dispersion relation for a constant surface temperature of the cylinder.

Sharma and Sharma [12] investigated the free vibration analysis of homogeneous transversely isotropic thermo elastic cylindrical panel. Asymptotic wave motion in transversely isotropic plates was analyzed by Sharma and Kumar [13]. Ashida and Tauchert [14] have presented the temperature and stress analysis of an elastic circular cylinder in contact with heated rigid stamps. Later, Ashida [15] presented the thermally - induced wave propagation in a piezoelectric plate. Tso and Hansen [16] have studied the wave propagation through cylinder/plate junctions. Heyliger and Ramirez [17] analyzed the free vibration characteristics of laminated circular piezoelectric plates and disc by using a discrete-layer model of the weak form of the equations of periodic motion. Thermal deflection of an inverse thermo elastic problem in a thin isotropic circular plate was presented by Gaikward and Deshmukh [18]. Varma [19] presented the propagation of waves in layered anisotropic media in generalized thermo elasticity in an arbitrary layered plate. Ponnusamy [20, 21] has studied, the wave propagation in a generalized thermo elastic homogeneous transversely isotropic thermo elastic solid cylinder of polygonal cross-sections using the Fourier expansion collocation method. Dispersion analysis of generalized magneto-thermoelastic waves in a transversely isotropic cylindrical panel and wave propagation in a generalized thermo elastic plate immersed in fluid respectively is analyzed by Ponnusamy and Selvamani [22, 23]. Jiangong et al. [25] discussed the circumferential thermo-elastic waves in orthotropic cylindrical curved plates without energy dissipation, Later, Yu Jiangong with Xue Tonglong [26] presented the propagation of thermo-elastic waves in orthotropic spherical curved plates subjected to stress-free, isothermal boundary conditions in the context of the Green–Naghdi (GN) generalized thermo-elastic theory (without energy dissipation). The theoretical formulation is based on the linear GN thermo-elastic theory. Yu Jiangong et al. [27] analyzed the wave propagation of generalized thermo-elastic waves in functionally graded plates without energy dissipation.

In this paper, flexural wave motion in a heat conducting thermo elastic doubly connected polygonal cross-sectional plate composed of homogeneous isotropic material is studied using the Fourier expansion collocation method based on Lord-Shulman (LS), Green-Lindsay (GL), Coupled Theory (CT) theories of thermo-elasticity. The solutions to the equations of motion for an isotropic medium is obtained by using the two dimensional theory of elasticity. It is assumed that, there is no vibration and displacement along the z-axis, that is the displacement along the z-axis, w is zero. The computed non-dimensional frequencies are compared with Lord-Shulman (LS), Green-Lindsay (GL) Coupled Theory (CT) theories of thermo-elasticity for flexural symmetric and flexural anti symmetric modes of vibrations and the frequencies are tabulated. The dispersion curves are drawn for thermally insulated and isothermal boundaries,

2. Formulation of the problem

We consider a homogeneous, isotropic, thermally conducting elastic doubly connected plate of polygonal cross-section with uniform temperature T_0 in the undisturbed state initially. The system displacements and stresses are defined by the polar coordinates r and θ in an arbitrary point inside the plate and denote the displacements u_r in the direction of r and u_θ in the tangential direction θ. The in-plane vibration and displacements of doubly connected arbitrary shaped plate is obtained by assuming that there is no vibration and displacement along the z-directions in the cylindrical coordinate system $\left(r,\theta,z\right)$. The two dimensional stress equations of motion, strain displacement relations and heat conduction equation in the absence of body forces for a linearly elastic medium are considered from Sharma and Sharma [12] as

$$\sigma_{rr,r}+r^{-1}\sigma_{r\theta,\theta}+r^{-1}\left(\sigma_{rr}-\sigma_{\theta\theta}\right)=\rho\ddot{u}_r$$

$$\sigma_{r\theta,r}+r^{-1}\sigma_{\theta\theta,\theta}+2r^{-1}\sigma_{r\theta}=\rho\ddot{u}_\theta, \tag{1}$$

$$K\left(T_{,rr}+r^{-1}T_{,r}+r^{-2}T_{,\theta\theta}\right)-\rho c_v\left(\dot{T}+t_0\ddot{T}\right)=T_0\left(\frac{\partial}{\partial t}+\delta_{1k}t_0\frac{\partial^2}{\partial t^2}\right)\left[\beta\left(u_{r,r}+r^{-1}\left(u_{\theta,\theta}+u_r\right)\right)\right], \tag{2}$$

and

$$\sigma_{rr}=\lambda\left(e_{rr}+e_{\theta\theta}\right)+2\mu e_{rr}-\beta\left(T+t_1\delta_{2k}\dot{T}\right),$$

$$\sigma_{\theta\theta}=\lambda\left(e_{rr}+e_{\theta\theta}\right)+2\mu e_{\theta\theta}-\beta\left(T+t_1\delta_{2k}\dot{T}\right), \tag{3}$$

$$\sigma_{r\theta}=2\mu e_{r\theta}, \tag{4}$$

where $\sigma_{rr},\ \sigma_{\theta\theta},\sigma_{r\theta}$ are the stress components, $e_{rr},e_{\theta\theta},e_{r\theta}$ are the strain components, T is the temperature change about the equilibrium temperature T_0, ρ is the mass density, c_v is the specific heat capacity, β is the thermal capacity factor that couples the heat conduction and elastic field equations, K is the thermal conductivity, $t_0,\ t_1$ are the two thermal relaxation times, t is the time, λ and μ are Lame's constants. The comma notation is used for spatial derivatives; the superposed dot represents time differentiation, and δ_{ij} is the Kronecker delta. In addition, k=1 for Lord-Shulman (LS) theory and k=2 for Green-Lindsay (GL) theory. The thermal relaxation times t_0 and t_1 satisfy the inequalities $t_0\ge t_1\ge 0$ for GL theory only and we assume that $\rho>0,\ T_0>0$, and $c_v>0$. The strain e_{ij} related to the displacements are given by

$$e_{rr}=u_{r,r},\ e_{\theta\theta}=r^{-1}\left(u_r+u_{\theta,\theta}\right),\ e_{r\theta}=u_{\theta,r}-r^{-1}\left(u_\theta-u_{r,\theta}\right). \tag{5}$$

3. Lord-Shulman (LS) theory

The Lord-Shulman theory of heat conduction equation for a two-dimensional theory of thermo-elasticity is obtained by substituting k=1 in the equations (2) and (3), we get

$$K\left(T_{,rr}+r^{-1}T_{,r}+r^{-2}T_{,\theta\theta}\right)-\rho c_v\left(\dot{T}+t_0\ddot{T}\right)=T_0\left(\frac{\partial}{\partial t}+t_0\frac{\partial^2}{\partial t^2}\right)\left[\beta\left(u_{r,r}+r^{-1}\left(u_{\theta,\theta}+u_r\right)\right)\right], \tag{6}$$

and

$$\sigma_{rr}=\lambda\left(e_{rr}+e_{\theta\theta}\right)+2\mu e_{rr}-\beta T,$$

$$\sigma_{\theta\theta}=\lambda\left(e_{rr}+e_{\theta\theta}\right)+2\mu e_{\theta\theta}-\beta T. \tag{7}$$

Substituting the Eqs. (4), (5) and (7) in Eqs. (1) and (6), the displacement equations of motions are obtained as

$$(\lambda+2\mu)\left(u_{r,rr}+r^{-1}u_{r,r}-r^{-2}u_r\right)+\mu r^{-2}u_{r,\theta\theta}+r^{-1}(\lambda+\mu)u_{\theta,r\theta}+r^{-2}(\lambda+3\mu)u_{\theta,\theta}-\beta T_{,r}=\rho\ddot{u}_r\,,$$

$$\mu\left(u_{\theta,rr}+r^{-1}u_{\theta,r}-r^{-2}u_\theta\right)+r^{-2}(\lambda+2\mu)u_{\theta,\theta\theta}+r^{-2}(\lambda+3\mu)u_{r,\theta}+r^{-1}(\lambda+\mu)u_{r,r\theta}-\beta T_{,\theta}=\rho\ddot{u}_\theta\,,$$

$$K\left(T_{,rr}+r^{-1}T_{,r}+r^{-2}T_{,\theta\theta}\right)-\rho c_v\left(\dot{T}+t_0\ddot{T}\right)-T_0\left(\frac{\partial}{\partial t}+t_0\frac{\partial^2}{\partial t^2}\right)\left[\beta\left(u_{r,r}+r^{-1}\left(u_{\theta,\theta}+u_r\right)\right)\right]. \tag{8}$$

3.1. Solution of the problem. Equation (8) is a coupled partial differential equation with two displacements and heat conduction components. To uncouple the Eq. (8), we follow the solutions from Mirsky [28] by assuming the vibration and displacements along the axial direction z is equal to zero, and assuming the solutions of the Eq. (8) in the form

$$u_r(r,\theta,t)=\sum_{n=0}^{\infty}\varepsilon_n\left[\left(\phi_{n,r}+r^{-1}\psi_{n,\theta}\right)+\left(\overline{\phi}_{n,r}+r^{-1}\overline{\psi}_{n,\theta}\right)\right]e^{i\omega t}\,,$$

$$u_\theta(r,\theta,t)=\sum_{n=0}^{\infty}\varepsilon_n\left[\left(r^{-1}\phi_{n,\theta}-\psi_{n,r}\right)+\left(r^{-1}\overline{\phi}_{n,\theta}-\overline{\psi}_{n,r}\right)\right]e^{i\omega t}\,,$$

$$T(r,\theta,t)=\left(\lambda+2\mu/\beta a^2\right)\sum_{n=0}^{\infty}\varepsilon_n\left(T_n+\overline{T}_n\right)e^{i\omega t}\,, \tag{9}$$

where $\varepsilon_n=\frac{1}{2}$ for n=0, $\varepsilon_n=1$ for $n\geq 1$, $i=\sqrt{-1}$, ω is the angular frequency, $\phi_n(r,\theta)$, $\psi_n(r,\theta)$, $T_n(r,\theta)$, $\overline{\phi}_n(r,\theta)$, $\overline{\psi}_n(r,\theta)$, and $\overline{T}_n(r,\theta)$ are the displacement potentials.

Introducing the dimensionless quantities such as

$\overline{\lambda}=\dfrac{\lambda}{\mu}$, $x=\dfrac{r}{a}$, $\tau_0=(1+t_0 i\omega)$, $\overline{K}=K\sqrt{\rho\mu}/\tau_0\beta^2 aT_0\Omega$, $\overline{d}=\rho c_v\mu/\beta^2 T_0$, $T_a=t\sqrt{\mu/\rho/a}$, $\tau_1=(1+t_1 i\omega)$, $c_i^2=(\lambda+2\mu)/\rho$, $\Omega^2=\omega^2a^2/c_1$, c_1^2 is the phase velocity.

Substituting Eq.(9) in Eq.(8), we obtain

$$\left\{(2+\lambda)\nabla^2+\Omega^2\right\}\phi_n-T_n=0\,,$$

$$\left\{\nabla^2\phi_n+\left(i\overline{K}\nabla^2+\overline{d}\right)T_n\right\}=0\,, \tag{10}$$

and

$$\left(\nabla^2+\Omega^2\right)\psi_n=0\,, \tag{11}$$

where $\nabla^2=\partial^2/\partial x^2+x^{-1}\,\partial/\partial x+x^{-2}\,\partial^2/\partial\theta^2$.

Eliminating T_n from the Eq. (10), we obtain

$$\left(A\nabla^4+B\nabla^2+C\right)\phi_n=0\,, \tag{12}$$

where

$$A = i\overline{K}_1\left(2+\overline{\lambda}\right), \quad B = \left\{(2+\lambda)\overline{d} + i\overline{K}\Omega^2 + 1\right\}, \; C = \Omega^2\overline{d}. \tag{13}$$

The solution of Eq. (12) for the symmetric mode is

$$\phi_n = \sum_{i=1}^{2}\left[A_{in}J_n\left(\alpha_i ax\right) + B_{in}Y_n\left(\alpha_i ax\right)\right]\cos n\theta$$

$$T_n = \sum_{i=1}^{2} a_i\left[A_{in}J_n\left(\alpha_i ax\right) + B_{in}Y_n\left(\alpha_i ax\right)\right]\cos n\theta, \tag{14}$$

where J_n is the Bessel function of first kind of order *n* and Y_n is the Bessel function of second kind of order *n*, $\left(\alpha_i a\right)^2$ are the roots of the equation $A\left(\alpha a\right)^4 - B\left(\alpha a\right)^2 + C = 0$ and the constant is

$$a_i = \left(\left(2+\overline{\lambda}\right)\nabla^2 + \Omega^2\right), i = 1, 2.$$

Solving Eq. (11), we get the solution for the symmetric mode as

$$\psi_n = \left[A_{3n}J_n\left(\alpha_3 ax\right) + B_{3n}Y_n\left(\alpha_3 ax\right)\right]\sin n\theta. \tag{15}$$

The solutions for the anti-symmetric mode $\overline{\phi}_n, \overline{T}_n$ and $\overline{\psi}_n$ are obtained from the Eqs. (14) and Eq. (15) by replacing $\sin n\theta$ by $\cos n\theta$ and $\cos n\theta$ by $\sin n\theta$. If $\left(\alpha_i a\right)^2 < 0$ (*i*=1, 2, 3), then the Bessel functions J_n and Y_n are to be replaced by the modified Bessel function I_n and K_n, respectively.

3.2. Boundary conditions and frequency equations. In this problem, the free vibration of doubly connected polygonal (triangle, square, pentagon and hexagon) cross-sectional plate is considered. Since the cross-section of the boundary is irregular in shape, it is difficult to satisfy the boundary conditions along the outer and inner surface of the plate directly. Hence, in the same line of Nagaya [1-5] the Fourier expansion collocation method is applied. Thus, the boundary conditions along the outer boundary of the plate is obtained as

$$\left(\sigma_{xx}\right)_i = \left(\sigma_{xy}\right)_i = \left(T_{,r} + hT\right)_i = 0, \tag{16}$$

and for the inner boundary, the boundary conditions are

$$\left(\sigma'_{xx}\right)_i = \left(\sigma'_{xy}\right)_i = \left(T'_{,r} + hT'\right)_i = 0, \tag{17}$$

where *h* is the surface heat transfer coefficient. Here $h \to 0$ corresponds to thermally insulated surface and $h \to \infty$ refers to isothermal one. Where *x* is the coordinate normal to the boundary and *y* is the coordinate tangential to the boundary, σ_{xx}, σ'_{xx} are the normal stresses, $\sigma_{xy}, \sigma'_{xy}$ are the shearing stresses; *T* and T' are the thermal fields, and $\left(\;\right)_i$ is the value at the $i-th$ segment of the outer and inner boundary respectively. If the angle γ_i, between the normal to the segment and the reference axis is assumed to be constant, then the transformed expression for the stresses are obtained following Nagaya [4] as

$$\sigma'_{xx} = \lambda\left(u_{r,r} + r^{-1}\left(u_r + u_{\theta,\theta}\right)\right) + 2\mu\{u_{r,r}\cos^2\left(\theta-\gamma_i\right) + r^{-1}\left(u_r + u_{\theta,\theta}\right)\sin^2\left(\theta-\gamma_i\right) +$$

$$+0.5\left(r^{-1}\left(u_{\theta}-u_{r,\theta}\right)-u_{\theta,r}\right)\sin 2\left(\theta-\gamma_{i}\right)\}-\beta T \,,$$

$$\sigma'_{xy}=\mu\left(u_{r,r}-r^{-1}\left(u_{\theta,\theta}+u_{r}\right)\sin 2\left(\theta-\gamma_{i}\right)+\left(r^{-1}\left(u_{r,\theta}-u_{\theta}\right)+u_{\theta,r}\right)\sin 2\left(\theta-\gamma_{i}\right)\right). \tag{18}$$

Substituting Eqs.(14), (15) in the Eqs.(16) and (17), and performing the Fourier series expansion to the boundary, the boundary condition along the inner and outer surfaces are expanded in the form of double Fourier series. When the plate is symmetric about more than one axis, the boundary conditions in the case of symmetric mode can be written in the form of a matrix as given below:

$$\begin{bmatrix}
\overset{1}{E}_{00} & \overset{2}{E}_{00} & \overset{3}{E}_{00} & \overset{4}{E}_{00} & \overset{1}{E}_{01} & \cdots & \overset{1}{E}_{0N} & \overset{2}{E}_{01} & \cdots & \overset{2}{E}_{0N} & \overset{3}{E}_{01} & \cdots & \overset{3}{E}_{0N} & \overset{4}{E}_{01} & \cdots & \overset{4}{E}_{0N} & \overset{5}{E}_{01} & \cdots & \overset{5}{E}_{0N} & \overset{6}{E}_{01} & \cdots & \overset{6}{E}_{0N} \\
\vdots & \vdots & \vdots & \vdots & \vdots & & \vdots & \vdots & & \vdots & \vdots & & \vdots & \vdots & & \vdots & \vdots & & \vdots & \vdots & & \vdots \\
\overset{1}{E}_{N0} & \overset{2}{E}_{N0} & \overset{3}{E}_{N0} & \overset{4}{E}_{N0} & \overset{1}{E}_{N1} & \cdots & \overset{1}{E}_{NN} & \overset{2}{E}_{N1} & \cdots & \overset{2}{E}_{NN} & \overset{3}{E}_{N1} & \cdots & \overset{3}{E}_{NN} & \overset{4}{E}_{N1} & \cdots & \overset{4}{E}_{NN} & \overset{5}{E}_{N1} & \cdots & \overset{5}{E}_{NN} & \overset{6}{E}_{N1} & \cdots & \overset{6}{E}_{NN} \\
\overset{1}{F}_{10} & \overset{2}{F}_{10} & \overset{3}{F}_{10} & \overset{4}{F}_{10} & \overset{1}{F}_{11} & \cdots & \overset{1}{F}_{1N} & \overset{2}{F}_{11} & \cdots & \overset{2}{F}_{1N} & \overset{3}{F}_{11} & \cdots & \overset{3}{F}_{1N} & \overset{4}{F}_{11} & \cdots & \overset{4}{\widehat{F}}_{1N} & \overset{5}{\widehat{F}}_{11} & \cdots & \overset{5}{\widehat{F}}_{1N} & \overset{6}{\widehat{F}}_{11} & \cdots & \overset{6}{\widehat{F}}_{1N} \\
\vdots & \vdots & \vdots & \vdots & \vdots & & \vdots & \vdots & & \vdots & \vdots & & \vdots & \vdots & & \vdots & \vdots & & \vdots & \vdots & & \vdots \\
\overset{1}{\widehat{F}}_{N0} & \overset{2}{\widehat{F}}_{N0} & \overset{3}{\widehat{F}}_{N0} & \overset{4}{\widehat{F}}_{N0} & \overset{1}{\widehat{F}}_{N1} & \cdots & \overset{1}{\widehat{F}}_{NN} & \overset{2}{\widehat{F}}_{N1} & \cdots & \overset{2}{\widehat{F}}_{NN} & \overset{3}{\widehat{F}}_{N1} & \cdots & \overset{3}{\widehat{F}}_{NN} & \overset{4}{\widehat{F}}_{N1} & \cdots & \overset{4}{\widehat{F}}_{NN} & \overset{5}{\widehat{F}}_{N1} & \cdots & \overset{5}{\widehat{F}}_{NN} & \overset{6}{\widehat{F}}_{N1} & \cdots & \overset{6}{\widehat{F}}_{NN} \\
\overset{1}{\widehat{G}}_{00} & \overset{2}{\widehat{G}}_{00} & \overset{3}{\widehat{G}}_{00} & \overset{4}{\widehat{G}}_{00} & \overset{1}{\widehat{G}}_{01} & \cdots & \overset{1}{\widehat{G}}_{0N} & \overset{2}{\widehat{G}}_{01} & \cdots & \overset{2}{\widehat{G}}_{0N} & \overset{3}{\widehat{G}}_{01} & \cdots & \overset{3}{\widehat{G}}_{0N} & \overset{4}{\widehat{G}}_{01} & \cdots & \overset{4}{\widehat{G}}_{0N} & \overset{5}{\widehat{G}}_{01} & \cdots & \overset{5}{\widehat{G}}_{0N} & \overset{6}{\widehat{G}}_{01} & \cdots & \overset{6}{\widehat{G}}_{0N} \\
\vdots & \vdots & \vdots & \vdots & \vdots & & \vdots & \vdots & & \vdots & \vdots & & \vdots & \vdots & & \vdots & \vdots & & \vdots & \vdots & & \vdots \\
\overset{1}{\widehat{G}}_{N0} & \overset{2}{\widehat{G}}_{N0} & \overset{3}{\widehat{G}}_{N0} & \overset{4}{\widehat{G}}_{N0} & \overset{1}{\widehat{G}}_{N1} & \cdots & \overset{1}{\widehat{G}}_{NN} & \overset{2}{\widehat{G}}_{N1} & \cdots & \overset{2}{\widehat{G}}_{NN} & \overset{3}{\widehat{G}}_{N1} & \cdots & \overset{3}{\widehat{G}}_{NN} & \overset{4}{\widehat{G}}_{N1} & \cdots & \overset{4}{\widehat{G}}_{NN} & \overset{5}{\widehat{G}}_{N1} & \cdots & \overset{5}{\widehat{G}}_{NN} & \overset{6}{\widehat{G}}_{N1} & \cdots & \overset{6}{\widehat{G}}_{NN} \\
E^{1}_{00} & E^{2}_{00} & E^{3}_{00} & E^{4}_{00} & E^{1}_{10} & \cdots & E^{1}_{0N} & E^{2}_{10} & \cdots & E^{2}_{0N} & E^{3}_{10} & \cdots & E^{3}_{0N} & E^{4}_{10} & \cdots & E^{4}_{0N} & E^{5}_{10} & \cdots & E^{5}_{0N} & E^{6}_{10} & \cdots & E^{6}_{0N} \\
\vdots & \vdots & \vdots & \vdots & \vdots & & \vdots & \vdots & & \vdots & \vdots & & \vdots & \vdots & & \vdots & \vdots & & \vdots & \vdots & & \vdots \\
E^{1}_{N0} & E^{2}_{N0} & E^{3}_{N0} & E^{4}_{N0} & E^{1}_{N1} & \cdots & E^{1}_{NN} & E^{2}_{N1} & \cdots & E^{2}_{NN} & E^{3}_{N1} & \cdots & E^{3}_{NN} & E^{4}_{N1} & \cdots & E^{4}_{NN} & E^{5}_{NN} & \cdots & E^{5}_{NN} & E^{6}_{N1} & \cdots & E^{6}_{NN} \\
F^{1}_{10} & F^{2}_{10} & F^{3}_{10} & F^{4}_{10} & F^{1}_{11} & \cdots & F^{1}_{1N} & F^{2}_{11} & \cdots & F^{2}_{1N} & F^{3}_{11} & \cdots & F^{3}_{1N} & F^{4}_{11} & \cdots & F^{4}_{1N} & F^{5}_{11} & \cdots & F^{5}_{1N} & F^{6}_{11} & \cdots & F^{6}_{1N} \\
\vdots & \vdots & \vdots & \vdots & \vdots & & \vdots & \vdots & & \vdots & \vdots & & \vdots & \vdots & & \vdots & \vdots & & \vdots & \vdots & & \vdots \\
F^{1}_{N0} & F^{2}_{N0} & F^{3}_{N0} & F^{4}_{N0} & F^{1}_{N1} & \cdots & F^{1}_{NN} & F^{2}_{N1} & \cdots & F^{2}_{NN} & F^{3}_{N1} & \cdots & F^{3}_{NN} & F^{4}_{N1} & \cdots & F^{4}_{NN} & F^{5}_{N1} & \cdots & F^{5}_{NN} & F^{6}_{N1} & \cdots & F^{6}_{NN} \\
G^{1}_{00} & G^{2}_{00} & G^{3}_{00} & G^{4}_{00} & G^{1}_{00} & \cdots & G^{1}_{0N} & G^{2}_{00} & \cdots & G^{2}_{0N} & G^{3}_{00} & \cdots & G^{3}_{0N} & G^{4}_{00} & \cdots & G^{4}_{0N} & G^{5}_{00} & \cdots & G^{5}_{0N} & G^{6}_{00} & \cdots & G^{6}_{0N} \\
\vdots & \vdots & \vdots & \vdots & \vdots & & \vdots & \vdots & & \vdots & \vdots & & \vdots & \vdots & & \vdots & \vdots & & \vdots & \vdots & & \vdots \\
G^{1}_{N0} & G^{2}_{N0} & G^{3}_{N0} & G^{4}_{N0} & G^{1}_{N1} & \cdots & G^{1}_{NN} & G^{2}_{N1} & \cdots & G^{2}_{NN} & G^{3}_{N1} & \cdots & G^{3}_{NN} & G^{4}_{N1} & \cdots & G^{4}_{N1} & G^{5}_{N1} & \cdots & G^{5}_{N1} & G^{6}_{N1} & \cdots & G^{6}_{NN}
\end{bmatrix}
\begin{bmatrix}
A_{10} \\ B_{10} \\ A_{20} \\ B_{20} \\ A_{11} \\ \vdots \\ A_{1N} \\ B_{11} \\ \vdots \\ B_{1N} \\ \vdots \\ \vdots \\ \vdots \\ \vdots \\ A_{31} \\ \vdots \\ A_{3N} \\ B_{31} \\ \vdots \\ B_{3N}
\end{bmatrix} = 0 \tag{19}$$

in which

$$\overset{j}{E}_{mn}=\left(2\varepsilon_{n}/\pi\right)\sum_{i=1}^{I}\int_{\theta_{i-1}}^{\theta_{i}} e_{n}^{j}\left(R_{i},\theta\right)\cos m\theta d\theta \,, \overset{j}{F}_{mn}=\left(2\varepsilon_{n}/\pi\right)\sum_{i=1}^{I}\int_{\theta_{i-1}}^{\theta_{i}} f_{n}^{j}\left(R_{i},\theta\right)\sin m\theta d\theta \,,$$

$$\overset{j}{G}_{mn}=\left(2\varepsilon_{n}/\pi\right)\sum_{i=1}^{I}\int_{\theta_{i-1}}^{\theta_{i}} g_{n}^{j}\left(R_{i},\theta\right)\cos m\theta d\theta \ , \ E_{mn}^{j}=\left(2\varepsilon_{n}/\pi\right)\sum_{i=1}^{I}\int_{\theta_{i-1}}^{\theta_{i}} e_{n}^{j}\left(R_{i},\theta\right)\cos m\theta d\theta \,,$$

$$F_{mn}^{j}=\left(2\varepsilon_{n}/\pi\right)\sum_{i=1}^{I}\int_{\theta_{i-1}}^{\theta_{i}} f_{n}^{j}\left(R_{i},\theta\right)\sin m\theta d\theta \,, G_{mn}^{j}=\left(2\varepsilon_{n}/\pi\right)\sum_{i=1}^{I}\int_{\theta_{i-1}}^{\theta_{i}} g_{n}^{j}\left(R_{i},\theta\right)\cos m\theta d\theta \,, \tag{20}$$

where $j=1,2,3,4,5$ and 6, I is the number of segments, R_{i} is the coordinate $\hat{r}$ at the inner boundary, R_{i} is the coordinate r at the outer boundary and N is the number of truncation of the Fourier series. The coefficients $e_{n}^{j} \sim \bar{g}_{n}^{j}$ are given in the Appendix A.

4. Green – Lindsay (GL) theory

The basic governing equations of motion and heat conduction in the absence of body force and heat source for a doubly connected polygonal cross-sectional plate, in the context of GL theory is obtained by substituting k=2 in the heat conduction Eq. (2) and in the stress-strain relation in Eq. (3), thus we obtain

$$K\left(T_{,rr}+r^{-1}T_{,r}+r^{-2}T_{,\theta\theta}\right)-\rho c_v\left(\dot{T}+t_0\ddot{T}\right)=T_0\frac{\partial}{\partial t}\left[\beta\left(u_{r,r}+r^{-1}\left(u_r+u_{\theta,\theta}\right)\right)\right], \tag{21}$$

and

$$\sigma_{rr}=\lambda\left(e_{rr}+e_{\theta\theta}\right)+2\mu e_{rr}-\beta\left(T+t_1\dot{T}\right). \tag{22}$$

Substituting the Eqs. (4), (5), (22) in the Eqs. (1) along with Eq.(21), we get the displacement equations of motion as follows:

$$\left(\lambda+2\mu\right)\left(u_{r,rr}+r^{-1}u_{r,r}-r^{-2}u_r\right)+\mu r^{-2}u_{r,\theta\theta}+r^{-1}\left(\lambda+\mu\right)u_{\theta,r\theta}+r^{-2}\left(\lambda+3\mu\right)u_{\theta,\theta}-\beta\left(T+t_1\dot{T}\right)_{,r}=\rho\ddot{u}_r,$$

$$\mu\left(u_{\theta,rr}+r^{-1}u_{\theta,r}-r^{-2}u_\theta\right)+r^{-2}\left(\lambda+2\mu\right)u_{\theta,\theta\theta}+r^{-2}\left(\lambda+3\mu\right)u_{r,\theta}+r^{-1}\left(\lambda+\mu\right)u_{r,r\theta}-\beta\left(T+t_1\dot{T}\right)_{,\theta}=\rho\ddot{u}_\theta,$$

$$K\left(T_{,rr}+r^{-1}T_{,r}+r^{-2}T_{,\theta\theta}\right)-\rho c_v\left(\dot{T}+t_0\ddot{T}\right)=T_0\left[\beta\left(u_{r,r}+r^{-1}\left(u_{\theta,\theta}+u_r\right)\right)\right]_{,t}. \tag{23}$$

The frequency equations for GL theory is obtained similarly as discussed in the previous section. The coefficients A, B and C are given by

$$A=iK_i\left(2+\overline{\lambda}\right),\ B=\left\{\left(2+\overline{\lambda}\right)\overline{d}+iK\Omega^2+\tau_1\right\},\ C=\Omega^2\overline{d}. \tag{24}$$

The Fourier coefficient $e_n^j \sim g_n^j$ are given in the Appendix A, the term a_i is to be replaced with b_i where $b_i=\left(\left(2+\overline{\lambda}\right)\nabla^2+\Omega^2\right)/\tau_1, i=1,2$.

5. Coupled theory (CT) of thermo-elasticity

The frequency equations for Coupled theory of thermo-elasticity are obtained by substituting the thermal relaxation times $t_0=t_1=0$ in the corresponding equation and solutions in the previous sections.

6. Uncoupled theory (UCT) of thermo-elasticity

The frequency equations for uncoupled theory of thermo elasticity are obtained by setting $\beta=K=c_v=T=T_0=0$ along with the thermo elastic coupling factors $t_0=t_1=0$ in the corresponding equations and solutions in the previous sections. Substituting $Y_n=Y_{n+1}=0$ in the frequency equation, the resulting frequency equation of a solid plate matches with the Eq. (26) of Ponnusamy [22].

7. Boundary conditions and frequency equation for rigidly fixed (clamped edge) boundary

The boundary conditions for rigidly fixed boundary is obtained by assuming the displacements along the radial direction u_r, along the circumferential direction u_θ and the thermal field T is equal to zero, thus we get the boundary for the outer surface as

$$\left(u_r\right)_i=\left(u_\theta\right)_i=\left(T\right)_i=0,$$

$$\left(u_r^{'}\right)_i=\left(u_\theta^{'}\right)_i=\left(T^{'}\right)_i=0, \text{ for the inner surface of the plate.} \tag{25}$$

Using the Eq. (9) in the Eq. (25), we can obtain the frequency equations for rigidly fixed boundary in the following form:

$$\left|b_{ij}\right| = 0, (i, j = 1,2,3,4,5,6), \tag{26}$$

where

$b_{1i} = \left\{nJ_n\left(\alpha_i ax\right) - \left(\alpha_i ax\right) J_{n+1}\left(\alpha_i ax\right)\right\}, i = 1,2$, $b_{13} = nJ_n\left(\alpha_3 ax\right)$,

$b_{2i} = nJ_n\left(\alpha_i ax\right), i = 1,2$, $b_{23} = \left\{nJ_n\left(\alpha_3 ax\right) - \left(\alpha_3 ax\right) J_{n+1}\left(\alpha_3 ax\right)\right\}$,

$b_{3i} = d_i J_n\left(\alpha_i ax\right), i = 1,2$, $b_{33} = 0$,

$b_{4i} = \left\{nJ_n\left(\alpha_i bx\right) - \left(\alpha_i bx\right) J_{n+1}\left(\alpha_i bx\right)\right\}$, $i = 1,2$, $b_{43} = nJ_n\left(\alpha_3 bx\right)$,

$b_{5i} = nJ_n\left(\alpha_i bx\right), i = 1,2$, $b_{53} = \left\{nJ_n\left(\alpha_3 bx\right) - \left(\alpha_3 bx\right) J_{n+1}\left(\alpha_3 bx\right)\right\}$,

$b_{6i} = d_i J_n\left(\alpha_i ax\right), i = 1,2$, $b_{63} = 0$.

The remaining terms $b_{ij}, b_{2j}, b_{3j}, b_{4j}, b_{5j}, b_{6j}, \left(j = 4,5,6\right)$ are obtained by replacing J_n and J_{n+1} with Y_n and Y_{n+1} respectively, and the constant $d_i = \left[\Omega^2 - \left(\alpha_i a\right)^2 \left(2 + \bar{\lambda}\right)\right]$.

8. Numerical results and discussion

The numerical analysis of the frequency equation is carried out for generalized thermo elastic doubly connected polygonal (square, triangle, pentagon and hexagon) cross-sectional plates, and the dimensions of each plate used in the numerical calculation are shown in Fig. 1. The axis of symmetry is denoted by the lines in the Fig. 1.

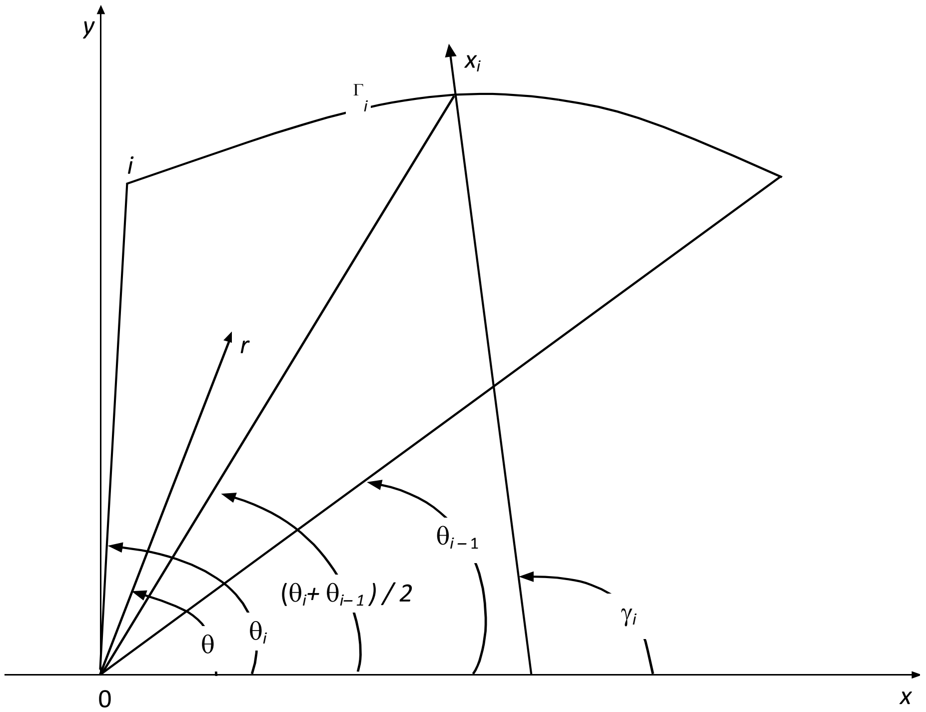

Fig. 1. Geometry of a straight line segment.

The material properties of copper at $42\,K$ are taken from Erbay and Suhubi [11] approximately as Poisson ratio $\nu = 0.3$, density $\rho = 8.96\times10^{3}kg/m^{3}$, the Young's modulus $E = 2.139\times10^{11}N/m^{2}$, $\lambda = 8.20\times10^{11}\,kg/ms^{2}$, $\mu = 4.20\times10^{10}\,kg/ms^{2}$, $c_{v} = 9.1\times10^{-2}\,m^{2}/ks^{2}$ and $K = 113\times10^{-2}\,kgm/ks^{2}$, and the thermal relaxation times considered from Sharma and Sharma [12] as $t_{0} = 0.75\times10^{-13}\sec$, $t_{1} = 0.5\times10^{-13}\sec$.

In the numerical calculation, the angle θ is taken as an independent variable and the coordinate R_i and R_i are at the $i-th$ segment of the boundary is expressed in terms of θ. Substituting R_i, R_i and the angle γ_i, between the reference axis and the normal to the $i-th$ boundary line, the integrations of the Fourier coefficients e_n^i, f_n^i, g_n^i, $\bar{e}_n^i$, $\bar{f}_n^i$, and $\bar{g}_n^i$ can be expressed in terms of the angle θ. Using these coefficients in to the equation (20), the frequencies are obtained for generalized thermo elastic polygonal plate.

8.1. Polygonal cross-sectional plate. The geometry of the ring shaped polygonal (triangle, square, pentagon and hexagon) cross-sectional plates are

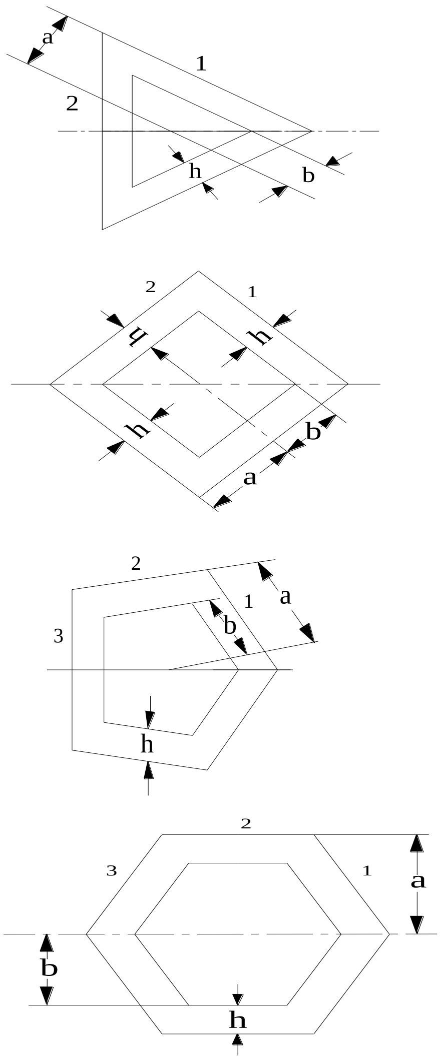

$\theta_0 = 0^\circ \quad \gamma_1 = 60^\circ$
$\theta_1 = 120^\circ \quad \gamma_2 = 180^\circ$
$\theta_2 = 180^\circ \quad I = 2$

(a)

$\theta_0 = 0^\circ \quad \gamma_1 = 45^\circ$
$\theta_1 = 90^\circ \quad \gamma_2 = 135^\circ$
$\theta_2 = 180^\circ \quad I = 2$

(b)

$\theta_0 = 0^\circ \quad \gamma_1 = 0^\circ$
$\theta_1 = 36^\circ \quad \gamma_2 = 72^\circ$
$\theta_2 = 108^\circ \quad \gamma_3 = 144^\circ$
$\theta_3 = 180^\circ \quad I = 3$

(c)

$\theta_0 = 0^\circ \quad \gamma_1 = 30^\circ$
$\theta_1 = 60^\circ \quad \gamma_2 = 72^\circ$
$\theta_2 = 120^\circ \quad \gamma_3 = 150^\circ$
$\theta_3 = 180^\circ \quad I = 3$

(d)

Fig. 2. Geometry of ring shaped polygonal plates.
(a) Triangle, (b) square, (c) pentagon, (d) hexagonal cross sections.

The geometrical relations for the polygonal cross-sectional doubly connected plates are given by Nagaya [2] as follows.

$$R_i/a = \left[\cos\left(\theta - \gamma_i\right)\right]^{-1},$$

$$R_i/b = \left[\cos\left(\theta - \gamma_i\right)\right]^{-1},\ \gamma_i = \gamma_i\ , \tag{27}$$

where $a(=b+h)$ and b is the apothems as shown in the Fig. 1, and h is the thickness of the plate. Here the apothem b is taken as the reference length which is used to obtain the dimensionless expressions, and γ_i is the angle between the reference axis and the normal to the segment. In the present problem, three kinds of basic independent modes of wave propagation have been considered, namely, the longitudinal and flexural anti symmetric modes of vibrations.

8.2. Flexural mode. In flexural mode of square and hexagonal cross-section, the vibration and displacements are anti symmetrical about the major axis and symmetrical about the minor axis. Hence the frequency equation may be obtained from Eq. (19) by changing $\cos n\theta$ by $\sin n\theta$ and $\sin n\theta$ by $\cos n\theta$ and choosing $n, m = 1,3,5,7...$. In the case of triangle and pentagonal cross-sections, the vibration and displacements are anti symmetrical about the minor axis, hence the frequency equations may be obtained by choosing $n, m = 1,2,3...$.

Since the boundary of the cross-sections namely, triangle, square, pentagon and hexagon are irregular, it is difficult to satisfy the boundary conditions along the curved surface, and hence Fourier expansion collocation method is applied. That is the curved surface, in the range $\theta = 0$ and $\theta = \pi$ is divided into 20 segments, such that the distance between any two segments is negligible and the integrations is performed for each segment numerically by using the Gauss five point formula .The non-dimensional frequencies are computed for $0 < \Omega \le 1.0$, using the secant method (applicable for the complex roots, Anita [29]).

To compare the results of the present method with that of the existing literature, the frequency equation of a thick polygonal cross-sectional plate without thermal field is chosen to show the agreement of the result obtained in the present case with the results of Nagaya [2]. The non-dimensional frequencies $|\Omega|$, obtained for a ring shaped polygonal plates, with clamped outside and inside edges, in both the Author and Nagaya's [2], have exact coincidence, which is shown in Table 1. Hence, the analysis was extended to understand the characteristics of vibration of the plate in thermal field. The notations namely, S_1, S_2, S_3 and A_1, A_2, A_3 used in the tables respectively represents the symmetric and anti symmetric modes of vibration, and the subscripts 1, 2, 3 represents the first, second and third modes of vibrations.

A comparison is made between the frequency response of different modes of vibration for GL, LS, CT and UCT theories of thermo elasticity for the flexural symmetric modes of triangular and pentagonal cross-sectional plates and is presented in Table 2, square and hexagonal cross-sectional plates is presented in Table 3. From the Tables 2, 3, it is observed that, as the modes of vibration increases, the non-dimensional frequencies also increase in the LS, GL and CT theories of thermo elasticity. Tables 4 and 5 represents the comparison between the frequencies of LS, GL, CT theories of thermo elasticity for the flexural anti symmetric modes of vibrations of triangle, square, pentagon and hexagonal cross-sectional plates. From the Tables 4 and 5 it is observed that as increasing the modes of vibrations, the non-dimensional frequency also increases in triangular, square, pentagonal and hexagonal cross-sectional plates.

Table 1. Comparison between the non-dimensional frequencies $|\Omega|$ of Author results with the results of Nagaya [2] of a ring shaped polygonal plates with clamped outside and clamped inside (ICOC) edges.

a/b	Mode	Triangle		Square		Pentagon		Hexagon	
		Nagaya	Author	Nagaya	Author	Nagaya	Author	Nagaya	Author
	S1	4.148	4.146	4.850	4.849	4.995	4.995	5.061	5.061
0.1	S2	4.392	4.393	4.997	4.997	5.132	5.132	5.163	5.162
	S3	4.547	4.551	5.889	5.886	5.627	5.626	5.784	5.783
	S1	4.269	4.267	5.128	5.127	5.297	5.296	5.367	5.365
0.15	S2	4.510	4.511	5.271	5.272	5.419	5.418	5.449	5.446
	S3	4.769	4.765	6.069	6.068	5.782	5.784	5.951	5.945
	S1	4.413	4.412	5.431	5.431	5.636	5.636	5.712	5.712
0.2	S2	4.622	4.613	5.573	5.572	5.742	5.741	5.771	5.772
	S3	4.924	4.924	6.315	6.316	5.995	5.996	6.180	6.181
	S1	4.474	4.573	5.757	5.756	6.018	6.017	6.103	6.103
0.25	S2	4.739	4.738	5.910	5.911	6.106	6.104	6.138	6.136
	S3	5.019	5.016	6.627	6.627	6.264	6.265	6.470	6.471

Table 2. Comparison between the non-dimensional frequencies $|\Omega|$ of Lord-Shulman (LS) Green-Lindsay (GL) and Coupled Theory (CT) theories of thermo-elasticity for flexural (symmetric) modes of triangular and pentagonal cross-sectional plates.

Mode		Triangle						Pentagon					
		LS		GL		CT		LS		GL		CT	
S1		4.2151		4.2403		4.3426		4.0076		4.0775		4.2511	
S2		4.8474		4.9872		4.8692		4.7112		4.8430		4.9522	
S3		5.5647		5.6966		5.6625		5.4685		5.4844		5.8029	
S4		6.2604		6.2625		6.3683		6.1122		6.1911		6.3618	
S5		6.9675		6.9685		7.0676		6.8276		6.8976		7.0225	

Table 3. Comparison between the non-dimensional frequencies $|\Omega|$ of Lord-Shulman (LS) Green-Lindsay (GL) and Coupled Theory (CT) theories of thermo-elasticity for flexural (symmetric) modes of square and hexagonal cross-sectional plates.

Mode		Square						Hexagon					
		LS		GL		CT		LS		GL		CT	
S1		4.2469		4.1053		4.2473		4.2469		4.2426		4.3841	
S2		4.9545		4.9501		5.0964		4.9511		4.9497		5.0927	
S3		5.6625		5.6556		5.8041		5.6624		5.6593		5.8041	
S4		6.3693		6.2288		6.3712		6.3668		6.2257		6.5118	
S5		7.0732		6.9290		7.2125		7.0680		6.9366		7.0704	

Table 4. Comparison between the non-dimensional frequencies $|\Omega|$ of the Lord-Shulman (LS) Green-Lindsay (GL) and Coupled Theory (CT) theories of thermo-elasticity for flexural (anti-symmetric) modes of triangular and pentagonal cross-sectional plates.

Mode	Triangle			Pentagon		
	LS	GL	CT	LS	GL	CT
A1	4.1440	4.1536	4.2475	4.0336	4.0978	4.2434
A2	4.8602	4.8621	4.9428	4.7134	4.8007	4.9526
A3	5.5753	5.5712	5.6615	5.4087	5.5055	5.6599
A4	6.2691	6.2785	6.3704	6.1590	6.2154	6.3711
A5	6.9696	6.9857	7.0715	6.8707	6.9220	7.0726

Table 5. Comparison between the non-dimensional frequencies $|\Omega|$ of Lord-Shulman (LS) Green-Lindsay (GL) and Coupled Theory (CT) theories of thermo-elasticity for flexural (anti symmetric) modes of square and hexagonal cross-sectional plates.

Mode	Square			Hexagon		
	LS	GL	CT	LS	GL	CT
A1	4.2377	4.1785	4.3766	4.2480	4.2232	4.3144
A2	4.9598	4.8095	5.0695	4.9535	4.8513	5.2585
A3	5.6645	5.5171	5.8027	5.6723	5.5509	5.8042
A4	6.3672	6.2246	6.3815	6.5083	6.1846	6.5117
A5	7.0761	6.9380	7.2124	7.0833	7.0781	7.2201

The non-dimensional frequency $|\Omega|$ of a ring shaped polygonal plate is obtained for various combinations of the outer and inner boundary conditions. To clarify the effect of the hole, the dispersion curves are drawn between the aspect ratio a/b versus the frequency $|\Omega|$. The solution for a doubly connected plate when aspect ratio a/b reduces to zero does not coincide with the solid plate, the fundamental frequency should be little lower than the case of solid plate, because the rigidity of the plate has decreased. This behavior is observed in all the graphs of longitudinal and flexural anti symmetric modes of vibrations. From all the graphs it can be noted that the first mode frequency first decreases and then increases with a/b when the plate has a hole. The effect of frequency of the inner boundary when it is clamped or simply supported is large compared with that of free edge boundary conditions.

8.3. Dispersion curves. The geometric relation for the polygonal cross-section is given in Eq. (27), which is used for the numerical calculation. The non-dimensional frequencies of flexural symmetric and anti symmetric modes are plotted in the form of dispersion curves as shown in the Figs. 3–10. The notations used in the Figures namely ICOF, IFOC and ICOC respectively denotes the Inner Clamped and Outer Free edges, Inner Free and Outer Clamped edges and Inner Clamped and Outer Clamped.

A graph is drawn for ICOF and IFOC edge boundary conditions between the wave number versus dimensionless frequency $|\Omega|$ for thermally insulated and isothermal boundary of triangular cross-sectional plates respectively which are shown in the graphs Fig. 3 and Fig. 4. From the Figs. 3 and 4, it is observed that, the non-dimensional frequency $|\Omega|$ increases with respect to its wave number, also it is noted that the frequency for ICOF surface have higher frequency than the frequency of IFOC edge boundary conditions. The frequencies increase for higher modes of vibrations, and the cross over points in the trend line indicates the transfer of heat energy between the modes of vibrations. The transfer of heat energy is linear in thermally insulated boundary as compared to the isothermal boundary.

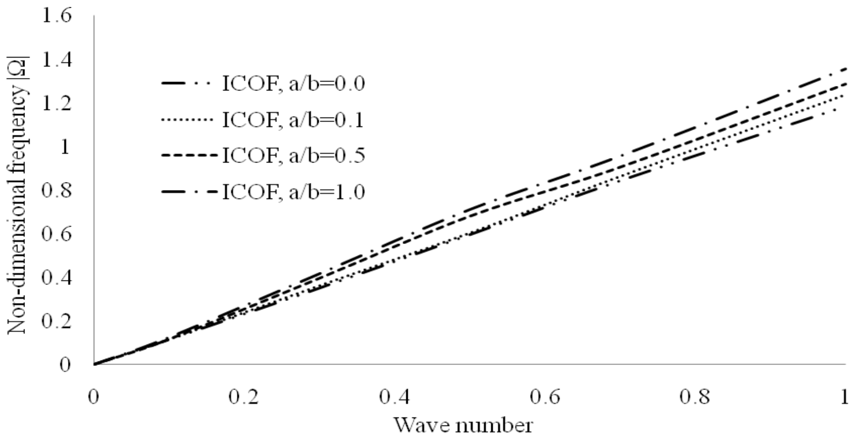

Fig. 3. Wave number versus non-dimensional frequency $|\Omega|$ for triangular cross-sectional plate with thermally insulated boundary.

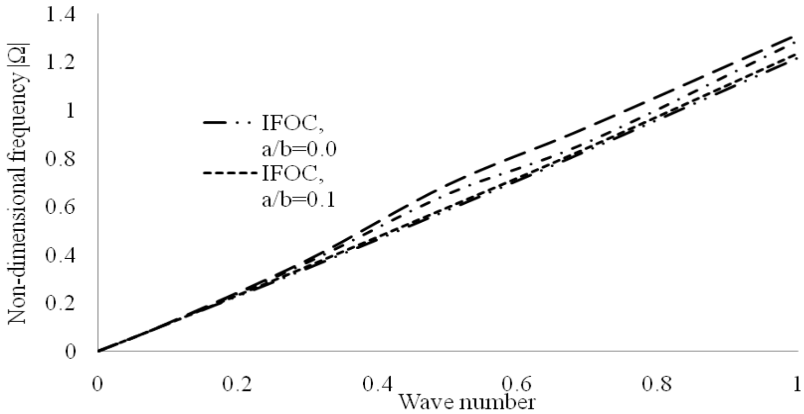

Fig. 4. Wave number versus non-dimensional frequency $|\Omega|$ for triangular cross-sectional plate with isothermal boundary.

A comparison is made between the non-dimensional frequency $|\Omega|$ and wave number for the thermally insulated and isothermal boundaries of square cross sectional plate is shown in Fig. 5 and Fig. 6.

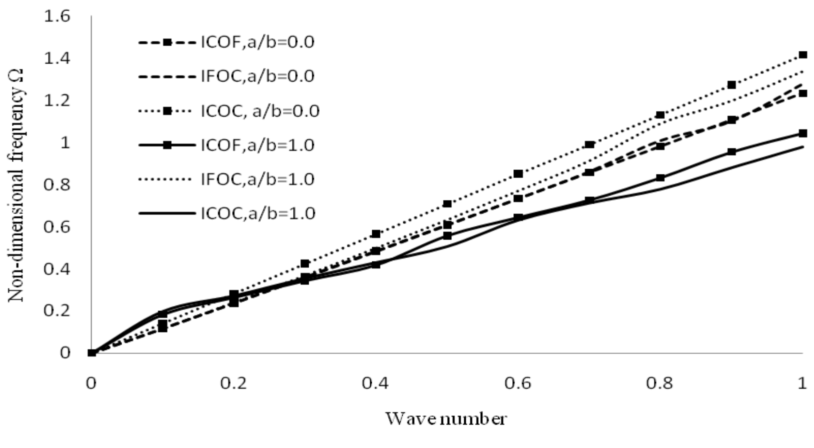

Fig. 5. Wave number versus non-dimensional frequency $|\Omega|$ of square cross-sectional plate with thermally insulated boundary.

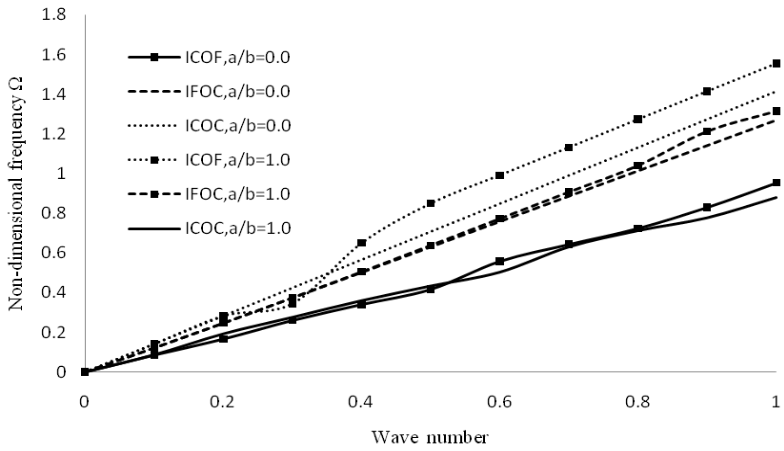

Fig. 6. Wave number versus non-dimensional frequency $|\Omega|$ of square cross-sectional plate with isothermal boundary.

From the Figs. 5 and 6, it is observed that the frequency is higher for a plate with both edges clamped as comparing with the other type of boundary conditions namely, ICOF and IFOC. The same physical behavior of a plate is obtained for the thermally insulated and isothermal modes of hexagonal cross-sectional plates which are shown in the Figs. 7 and 8, respectively.

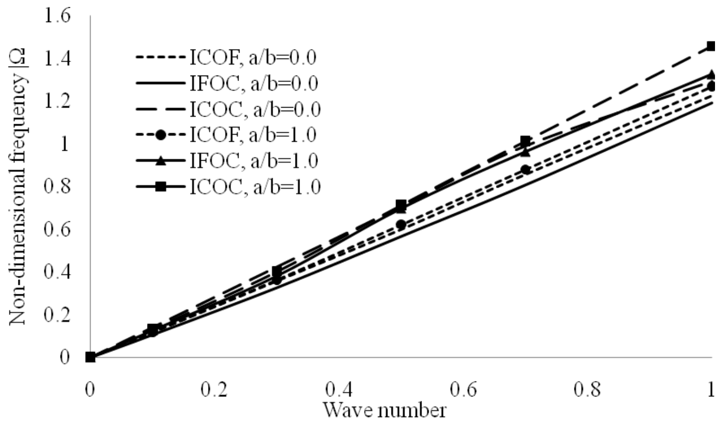

Fig. 7. Wave number versus non-dimensional frequency $|\Omega|$ of pentagonal cross-sectional plate with thermally insulated boundary.

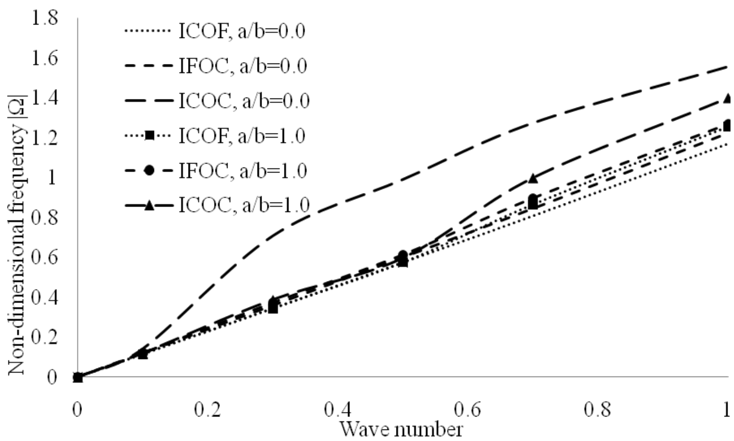

Fig. 8. Wave number versus non-dimensional frequency $|\Omega|$ of pentagonal cross-sectional plate with isothermal boundary.

From the Figs. 9 and 10, it is observed that the dispersions behavior of hexagonal plate is same in starting wave number range and dispersed in the higher wave number. The crosses over points denote the transfer of heat energy between the modes of vibrations. We have shown that the frequencies depend strongly on the cross-sections of the plate and deviate from the circular one. The dispersion curves of higher wave numbers are sensitive to the nature of the thermal boundary condition as well as to the measure of the thermo-mechanical cross-coupling for both propagating and evanescent waves. These dispersions curves obtained from the exact solution of the problem could be used as references data for developing of reliable finite elements and boundary elements for approximate solution of the problems of wave propagation in structures with moving heat sources.

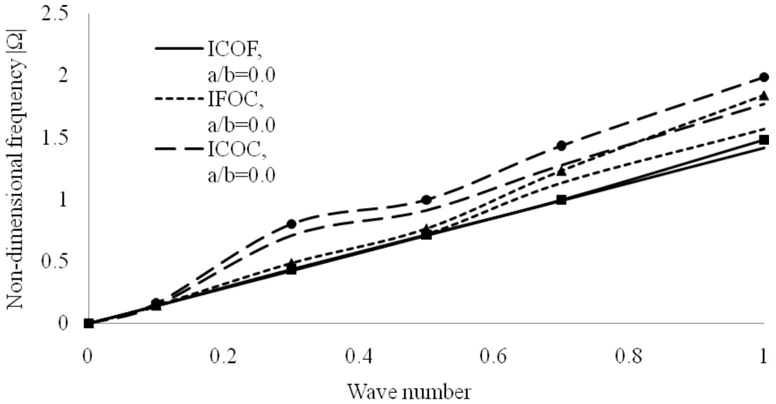

Fig. 9. Wave number versus non-dimensional frequency $|\Omega|$ of hexagonal cross-sectional plate with thermally insulated boundary.

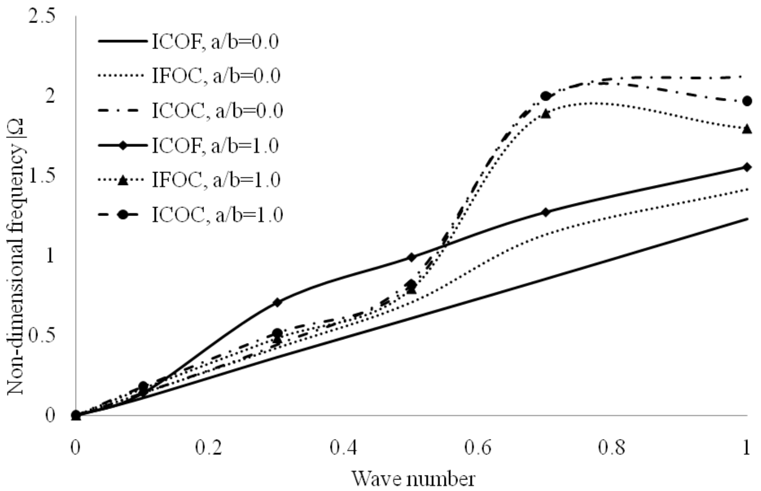

Fig. 10. Wave number versus non-dimensional frequency $|\Omega|$ of hexagonal cross-sectional plate with isothermal boundary.

9. Conclusions

Flexural wave motion in a heat conducting thermo elastic doubly connected polygonal cross-sectional plate is studied using the Fourier expansion collocation method. The equations of motion based on two-dimensional theory of elasticity is applied under the plane strain assumption of generalized thermo elastic plate of polygonal cross-sections composed of homogeneous isotropic material. The frequency equations are obtained by satisfying the boundary conditions along the inner and outer surface of the polygonal plate. The numerical calculations are carried out for triangular, square, pentagonal and hexagonal cross sectional plates. The computed non-dimensional frequencies are compared with the Lord-Shulman (LS), Green-Lindsay (GL), Coupled Theory (CT) theories of thermo-elasticity and they are presented in Tables. The dispersion curves are drawn for thermally insulated and isothermal boundaries.

Appendix A

The expressions $e_n^i \sim g_n^i$ used in Eq. (20) are given as follows:

$$e_n^i = 2\left\{n(n-1)J_n(\alpha_i ax)+(\alpha_i ax)J_{n+1}(\alpha_i ax)\right\}\cos 2(\theta-\gamma_i)\cos n\theta$$
$$-\ x^2\left\{(\alpha_i a)^2+\left[\overline{\lambda}+2\cos^2(\theta-\gamma_i)\right]+a_i\right\}J_n\left(\alpha_i ax\right)\cos n\theta$$
$$+2n\left\{(n-1)J_n(\alpha_i ax)-(\alpha_i ax)J_{n+1}(\alpha_i ax)\right\}\sin n\theta\sin 2(\theta-\gamma_i),\quad i=1,2\,; \tag{A1}$$

$$e_n^3 = 2\left\{n(n-1)J_n(\alpha_3 ax)-(\alpha_3 ax)J_{n+1}(\alpha_3 ax)\right\}\cos n\theta\ \ \cos 2(\theta-\gamma_i)$$
$$+2\left\{[n(n-1)-(\alpha_3 ax)^2]J_n(\alpha_3 ax)+(\alpha_3 ax)J_{n+1}(\alpha_3 ax)\right\}\sin n\theta\sin 2(\theta-\gamma_i)\,; \tag{A2}$$

$$e_n^4 = 2\left\{n(n-1)Y_n(\alpha_4 ax)-(\alpha_4 ax)Y_{n+1}(\alpha_4 ax)\right\}\cos n\theta\ \ \cos 2(\theta-\gamma_i)$$
$$+2\left\{[n(n-1)-(\alpha_4 ax)^2]Y_n(\alpha_4 ax)+(\alpha_4 ax)Y_{n+1}(\alpha_4 ax)\right\}\sin n\theta\sin 2(\theta-\gamma_i)\,; \tag{A3}$$

$$e_n^i = 2\left\{n(n-1)Y_n(\alpha_i ax)+(\alpha_i ax)Y_{n+1}(\alpha_i ax)\right\}\cos 2(\theta-\gamma_i)\cos n\theta$$
$$-\ x^2\left\{(\alpha_i a)^2+\left[\overline{\lambda}+2\cos^2(\theta-\gamma_i)\right]+a_i\right\}Y_n\left(\alpha_i ax\right)\cos n\theta$$
$$+2n\left\{(n-1)Y_n(\alpha_i ax)-(\alpha_i ax)Y_{n+1}(\alpha_i ax)\right\}\sin n\theta\sin 2(\theta-\gamma_i),\quad i=5,6\,; \tag{A4}$$

$$f_n^i = 2\left\{[n(n-1)-(\alpha_i ax)^2]J_n(\alpha_i ax)+(\alpha_i ax)J_{n+1}(\alpha_i ax)\right\}\cos n\theta\sin 2(\theta-\gamma_i)$$
$$+\ \ 2n\left\{(\alpha_i ax)J_{n+1}(\alpha_i ax)-(n-1)J_n(\alpha_i ax)\right\}\sin n\theta\cos 2(\theta-\gamma_i)\,,\ i=1,2\,; \tag{A5}$$

$$f_n^3 = 2n\left\{(n-1)J_n(\alpha_3 ax)-(\alpha_3 ax)J_{n+1}(\alpha_3 ax)\right\}\cos n\theta\sin 2(\theta-\gamma_i)$$
$$-\left\{2(\alpha_3 ax)J_{n+1}(\alpha_3 ax)-[(\alpha_3 ax)^2-2n(n-1)]J_n(\alpha_3 ax)\right\}\sin n\theta\cos 2(\theta-\gamma_i)\,; \tag{A6}$$

$$f_n^4 = 2n\left\{(n-1)Y_n(\alpha_4 ax)-(\alpha_4 ax)Y_{n+1}(\alpha_4 ax)\right\}\cos n\theta\sin 2(\theta-\gamma_i)$$
$$-\left\{2(\alpha_4 ax)Y_{n+1}(\alpha_4 ax)-[(\alpha_4 ax)^2-2n(n-1)]Y_n(\alpha_4 ax)\right\}\sin n\theta\cos 2(\theta-\gamma_i)\,; \tag{A7}$$

$$f_n^i = 2\left\{[n(n-1)-(\alpha_i ax)^2]Y_n(\alpha_i ax)+(\alpha_i ax)Y_{n+1}(\alpha_i ax)\right\}\cos n\theta\sin 2(\theta-\gamma_i)$$
$$+\ \ 2n\left\{(\alpha_i ax)Y_{n+1}(\alpha_i ax)-(n-1)Y_n(\alpha_i ax)\right\}\sin n\theta\cos 2(\theta-\gamma_i)\,,\ i=5,6\,; \tag{A8}$$

$$k_n^i = d_i\left\{n\cos\left(\overline{n-1}\theta+\gamma_i\right)J_n\left(\alpha_i ax\right)-\left(\alpha_i ax\right)J_{n+1}\left(\alpha_i ax\right)\cos(\theta-\gamma_i)\cos n\theta\right\},\ i=1,2\,; \tag{A9}$$

$$k_n^3 = 0.0\,,\ k_n^4 = 0.0\,; \tag{A10}$$

$$k_n^i = d_i \left\{ n\cos\left(\overline{n-1}\theta+\gamma_i\right)Y_n\left(\alpha_i ax\right)-\left(\alpha_i ax\right)Y_{n+1}\left(\alpha_i ax\right)\cos(\theta-\gamma_i)\cos n\theta \right\},\ i=5,6. \qquad \text{(A11)}$$

The expressions $\bar{e}_n^i \sim \bar{g}_n^i$ are obtained by replacing $\cos n\theta$ by $\sin n\theta$ and $\sin n\theta$ by $\cos n\theta$ in the Eqs. (A1) - (A11).

References

[1] K. Nagaya // *Journal of Sound and Vibration* **74(4)** (1981) 543.
[2] K. Nagaya // *Journal of Sound and Vibration* **74(4)** (1981) 553.
[3] K. Nagaya // *Journal of Acoustical Society of America* **70(3)** (1981) 763.
[4] K. Nagaya // *Journal of Applied Mechanics* **50** (1983) 757.
[5] K. Nagaya // Journal of Acoustical Society of America **74(5)** (1983) 1441.
[6] H.W. Lord, Y. Shulman // *Journal of Mechanics of Physics of Solids* **5** (1967) 299.
[7] R.S. Dhaliwal, H.H. Sherief // *Quartely Journal of Applied Mathematics* **8(1)** (1980) 1.
[8] A.E. Green, N. Laws // *Archive Rational Mechanical Analysis* **45**(1972) 47.
[9] A.E. Green, K.A. Lindsay // *Journal of Elasticity* **2** (1972) 1.
[10] E.S. Suhubi // *Journal of Mechanics of Physics of Solids* **12** (1964) 69.
[11] E.S. Erbay, E.S. Suhubi // *Journal of Thermal Stresses* **9** (1986) 279.
[12] J.N. Sharma, P.K. Sharma // *Journal of Thermal Stresses* **25** (2002) 169.
[13] J.N. Sharma, R. Kumar // *Journal of Sound and Vibration* **274** (2004) 747.
[14] F. Ashida, T.R. Taucher // *International Journal of Solids and Structures* **30** (2001) 4969.
[15] F. Ashida // *Acta Mechanica* **161** (2003) 1.
[16] Y.K. Tso, C.H. Hansen // *Journal of Sound and Vibration* **186(3)** (1995) 447.
[17] P.R. Heyliger, G. Ramirez // *Journal of Sound and Vibration* **229(4)** (2000) 935.
[18] M.K. Gaikward, K.C. Deshmukh // *Journal of Applied Mathematical Modeling* **29** (2005) 797.
[19] K.L. Varma // *International Journal of Engineering Sciences* **40** (2002) 2077.
[20] P. Ponnusamy // *International Journal of Solids and Structures* **44** (2007) 5336.
[21] P. Ponnusamy // *Journal of Applied Mathematical Modeling* **36** (2012) 3343.
[22] R. Selvamani, P. Ponnusamy // *Structural Engineering Mechanics* **46(6)** (2031) 827.
[23] P. Ponnusamy, R. Selvamani // Journal of thermal stresses **35** (2012) 1119.
[24] Yu Jiangong, Wu Bin, He Cunfu // *Ultrosonics* **53(3) (**2010) 416.
[25] Yu Jiangong, Xue Tonglong // *Acta Mechanica* **212** (2010) 39.
[26] Yu Jiangong, Zhang Xiaoming, Xue Tonglong // *Composite Structures* **93(1) ()** 32.
[27] I. Mirsky // *Journal of Acoustical Society of America* **37(6)** (1964)1016.
[28] H.M. Antia, *Numerical Methods for Scientists and Engineers* (Hindustan Book Agency, 2012).